*International Journal of Remote Sensing*
Vol. 32, No. 11, 10 June 2011, 3043–3053

# Observations of the ultra-fast Kelvin wave in the tropical mesosphere during equinox

A. GUHARAY*†, P. PANT‡, B. PANDE§ and K. PANDEY§
†Space and Atmospheric Sciences Division, Physical Research Laboratory, Navarangpura, Ahmedabad, India
‡Atmospheric Sciences Division, Aryabhatta Research Institute of Observational Sciences, Nainital, India
§Department of Physics, DSB Campus, Kumaun University, Nainital, India

Regular and systematic measurements of mesospheric temperatures have been carried out during March and April 2007 to determine planetary-scale wave activities in the tropical region, utilizing ground-based Rayleigh Light Detection and Ranging (LiDAR) and satellite-based Microwave Limb Sounder (MLS) data from Gadanki, India (13.5° N, 79.2° E) and MLS data over a site in North America (23.5° N, 100° W). A dominant component of the 3–5 day period wave is revealed at four altitudes (80, 70, 60 and 50 km) over the two observation stations. The estimated vertical wavelength (~40 km), zonal phase speed (~140 m $s^{-1}$), longitudinal and latitudinal extensions have suggested the wave to be an ultra-fast Kelvin (UFK) wave with zonal wave number 1. In addition to the UFK wave, a probable quasi 2 day Rossby gravity wave is also found to be present most of the time. Another 5–7 day wave component, observed at some altitudes with significant prominence, is surmised to be a manifestation of a 6.5 day wave.

## 1. Introduction

The fourth Intergovernmental Panel on Climate Change (Cracknell and Varotsos 2007) assessment report summarizes that although we have acquired significant knowledge on the climate variability and consequences to its changes for the last couple of years, there are still a number of unresolved problems in the perspective of physical–chemical–dynamical processes transpiring in the Earth's system, and to address these unsolved issues, we should take into account the long-term non-linear atmosphere–ocean–land, surface–cryosphere–biosphere interactions in the improved prediction models (Cracknell and Varotsos 2007).

Planetary-scale waves are supposed to be very significant contributors to the total energy budget of the Earth's atmosphere. They carry energy and momentum in course of their propagation, which are distributed in all latitudes and longitudes all around the globe throughout the seasons, from the lower atmosphere to the upper atmosphere and, consequently, give rise to large-scale wave activities. Using three-dimensional stratospheric dynamics and photochemistry model, Fusco and Salby (1999) showed significant inter-annual variability of the ozone concentration (ozone is an important trace species to control climate change and air quality) due to upward progressing

*Corresponding author. Email: guharay@in.com

*International Journal of Remote Sensing*
ISSN 0143-1161 print/ISSN 1366-5901 online 
http://www.tandf.co.uk/journals
DOI: 10.1080/01431161.2010.541522

planetary waves, hence, planetary waves are found to be indirectly responsible for climate change. Stationary planetary waves are very important drivers of equinox transition in the mesosphere (Liu *et al.* 2001). It has also been observed that inter-annual variability caused by planetary-wave breaking is closely associated with well-known modes (e.g. El Niňo Southern Oscillation, North Atlantic Oscillation) of climate variability (Abatzoglou and Magnusdottir 2006). Because of their considerable influence on global-scale dynamics and climate change, they have been studied for the last couple of decades by several investigators with the help of observations (Vincent 1993, Takahashi *et al*. 2006) and theoretical studies (Salby *et al*. 2007). Varotsos (1987) pointed out the dominant role of quasi-stationary planetary waves in the upper stratosphere and mesosphere during winter from a high-latitude site (60° N), which caused significant differences between the derived temperatures obtained from two reference atmosphere models. From the space-based observations of the High Resolution Doppler Imager (HRDI) on board the Upper Atmospheric Research Satellite (UARS), Wu *et al.* (1994) observed a 5 day wave in the 50–100 km region, and found good agreement with the Rossby normal (1,1) mode in both zonal and meridional winds. Pancheva *et al*. (2004) observed a quasi 2 day wave in the meridional wind component and a 3–7 day wave in the zonal wind data using meteor radar observations from a low-latitude site of the southern hemisphere (SH).

Varotsos (2003) suggested that a nearly 10 day component in the zonal mean temperature and wind at high latitudes of the SH, which seems to originate in the upper stratosphere, might be of crucial importance for the occurrence of the unprecedented event of the major, sudden stratospheric warming and the ozone hole split over Antarctica on 25 September 2002 (Varotsos 2002, 2004a,b).

A Kelvin wave (KW) is a special type of planetary wave that is different from Rossby normal modes. It is mainly trapped in the equatorial region where solar insolation is higher and Coriolis drag is less than in the mid and high latitudes. The KW was first observed by Wallace and Kousky (1968) in the stratosphere based on radiosonde data, and in the mesosphere, it was first investigated by Vincent (1993) using wind data obtained from the Medium Frequency (MF) radar. It was mostly created by large-scale tropospheric convection due to latent heat release (Holton 1972). After generation, it propagates along the equator from the lower to the upper atmosphere. It can be observed in the zonal wind, vertical wind, temperature, pressure, etc., with zonal wave number 1 and 2, but it cannot be observed in the meridional wind (Andrews *et al*. 1987). Depending upon the wave parameters, KWs are normally classified in three categories: slow (SK), fast (FK) and ultra-fast (UFK) waves. The SK wave is mostly observed in the lower atmosphere with a phase speed ~20–30 m $s^{-1}$, with a vertical wavelength ~10 km and a period ~16–20 days; there is much less possibility of observing it in the mesosphere and thermosphere. The FK wave is observed in the stratosphere and lower mesosphere with a phase speed ~50–70 m $s^{-1}$, a vertical wavelength ~20 km and a period ~6–9 days. The most dynamic KW, the UFK wave, can propagate up to the mesosphere and lower thermosphere due to high vertical wavelengths, which are greater than 40 km with a phase speed greater than 130 m $s^{-1}$and a period ~3–5 days (Takahashi *et al*. 2002).

Significant impacts of KWs through the zonal mean flow acceleration of the equatorial atmosphere can produce a remarkable variability in the stratospheric and mesospheric semi-annual oscillations (SSAOs and MSAOs), as well as stratospheric quasi-biennial oscillations (SQBOs) (Hitchman and Leovy 1988, Holton *et al.*

2001). Although several observational and model studies have been performed, our knowledge regarding this peculiar and unique wave feature is still not complete.

In the above perspective, we would like to point out the existence of the UFK wave in the tropical mesospheric region based on ground-based Rayleigh Light Detection and Ranging (LiDAR) and satellite-based Microwave Limb Sounder (MLS) temperature observations carried out mainly from two sites during the spring equinox period. Data from March and April of the year 2007 have been used for this purpose, and the results are obtained by performing wavelet and digital filter analysis. The observed parameter values and characteristics of propagation bear out the presence of the UFK wave.

## 2. Instruments and observations

We have used the nocturnal temperature data from the Rayleigh LiDAR, which actually utilizes a pulsed Nd:YAG laser with a pulse width ~7 nm and an average pulse energy of 550 mJ, operating at 532 nm. The LiDAR operation is conducted by the National Atmospheric Research Laboratory (NARL), Gadanki (13.5° N, 79.2° E) during cloud-free nights. In the Rayleigh mode, it can receive photon counts in the 30–90 km range with the help of a Newtonian telescope. The backscattered signal is proportional to the number density of the air molecules present, and hence, it is used to calculate the temperature with an altitude resolution of 300 m by applying the ideal gas law and assuming hydrostatic equilibrium in the atmosphere. The algorithm for temperature determination is similar to that of Hauchecorne and Chanin (1980). A detailed description of the analysis and technical specifications are given elsewhere (e.g. Siva Kumar *et al.* 2003).

The MLS, one of the four instruments on board the Aura satellite of the Earth Observing System (EOS), was launched on 15 July 2004. It measures limb emissions at 47 pressure levels ($10^3$–$10^{-5}$ hPa), starting from the troposphere to the thermosphere. Thermal microwave emissions from the atmospheric gases in the frequency range 115 GHz to 2.5 THz are used to obtain a total of ~3500 vertical profiles (240 profiles per orbit) of temperature, pressure, cloud, ice, etc. per day. In the mesosphere, it can measure temperature with a precision of ~3 K (at 0.001 hPa). It has a vertical resolution of ~3 km at 31.6 hPa, ~6 km at 316 hPa and ~13 km at 0.001 hPa (Schwartz *et al.* 2008). Comparison and validation of the MLS with other existing observations have been carried out by Schwartz *et al*. (2008). For our present purpose, we have used version 2.2 level 2 temperature data centred over Gadanki within a square latitude and longitude grid of ± 10° (to achieve vertical profiles for each day to minimize the data gap).

We have chosen LiDAR data from 19 March to 18 April 2007, a total of 31 nights with 5 days of data gaps distributed unevenly over the span. The reason for choosing this time period is the continuous and consistent receipt of data with a small number of data gaps (not more than one), which is not possible for other times. The nocturnal mean temperature profiles (on average 60–120 profiles over 4–8 hours observation spans per night) are obtained to get temperatures at 80, 70, 60 and 50 km altitudes. Similarly, the MLS data (on average 12–14 profiles received in few milliseconds on the particular night) are used for March and April 2007 for 60 days, with only a 1 day data gap at four pressure levels (0.01, 0.05, 0.2 and 0.5 hPa) corresponding to the four altitudes mentioned previously over Gadanki and North America (23.5° N, 100° W). The data gaps are filled with linear interpolation for both LiDAR and MLS measurements before carrying out any conclusive analysis.

## 3. Results

Figure 1 shows day to day variation of the mesospheric temperature pattern with respect to the corresponding day of the year (DY) at four altitudes selected for the present study during the spring equinox period, starting from 2 March to 30 April for the LiDAR and MLS. The LiDAR-obtained values show higher variability in comparison with the MLS-observed ones, perhaps due to the retrieval algorithms used for the temperature estimate or limitations and associated errors. Another important reason for this difference may be the spatial and temporal averaging interval. In the case of LiDAR, we have considered the nightly (few hours) average vertical profiles over a particular location (Gadanki), and in the case of MLS, an average snapshot of the vertical profiles during the overpass of the satellite over the latitude and longitude grid of ± 10° is considered, which may cause such discrepancies. The temperature variability obtained from both instruments increases with altitude because of several kinds of gravity waves and tidal activities. It is interesting to note that a 3–5 day wave is prominent in the LiDAR and MLS temperatures. In addition, there are other wave features that exist during certain times of the investigation span. As confirmative characteristics of UFK waves (3–5 day) is the theme of our present study, we shall only concentrate on this aspect in detail in the following sections.

For further verification of the UFK wave, we have carried out wavelet analysis using a Morlet wavelet as a mother wavelet on the time-series temperature data of the LiDAR at Gadanki. Details of the wavelet analysis procedure are given by Torrence

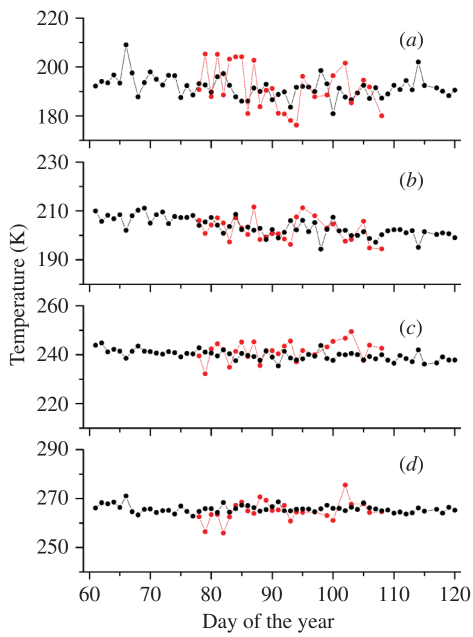


Figure 1. Temperature variability plot of LiDAR (red) and MLS (black) during the March to April 2007 period for: (*a*) 80 km, (*b*) 70 km, (*c*) 60 km and (*d*) 50 km over Gadanki.

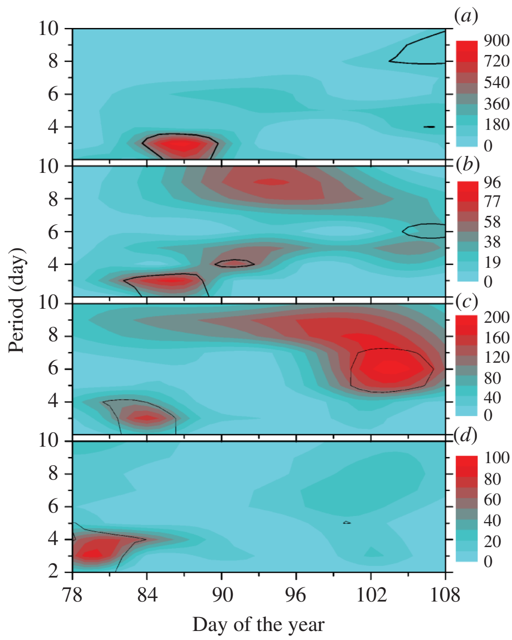


Figure 2. Wavelet power spectra of LiDAR temperature over Gadanki with respect to day of the year (DY) and period for: (*a*) 80 km, (*b*) 70 km, (*c*) 60 km and (*d*) 50 km. The solid lines represent the 90% significance level.

and Compo (1998). The normalized wavelet power spectra at four altitudes are shown in the contour plot in figure 2. The solid lines in the plot represent 90% significance level. Spectacular wave signatures come out from the spectra in the periodicity range 2–10 days. It is evident from the plot that 2–4 day periodicity oscillations are present all the time. There are clear phase shifts between the respective wave occurrences at various altitudes. An observed 4 day wave is dominant at 50 km at around 78–84 DY. At 60 km, an evident 3 day component is present during 82–86 DY, and a significant 5–7 day wave is present around 100–107 DY. The wave structure is a little bit different at 70 km, where a 2–3 day wave reveals its prominence around 83–89 DY. In addition, a 4 day component is observed ~90–93 DY, and a 6 day wave is visible around 105–108 DY. Again at 80 km, a 2–3.5 day wave appears during ~84–90 DY as well as a less prominent 8–10 day component present for a few days at the end. The 3–4 day wave component clearly shows upward wave propagation with time, as evident from the contours. The vertical wavelength, calculated from the time differences of the occurrence of 3–5 day wave contours for various altitudes, comes out to be ~40 km. Hence, the observed 3–4 day oscillation may be a UFK wave.

In order to study the latitudinal and longitudinal characteristics (or extension) of the propagating possible UFK wave, we have chosen another site of observation in North America (23.5° E, 100° W) using the MLS temperature data (within the latitude and longitude grid of ± 10°) and carried out the same wavelet analysis as described in the previous paragraph, which is shown in figure 3, at the same four altitude regions, from 2 March to 30 April 2007. An evident component of the 3.5–7 day period wave is observed at 50 km during the first few days of the month of March, and a 3 day

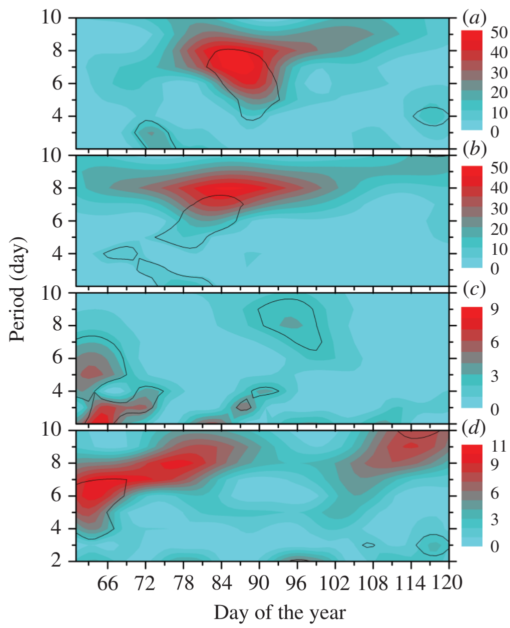


Figure 3. Same as figure 2, but this is for a site (23.5° N, 100° W) in North America using MLS data.

wave dominates on 108 and 115–120 DY. At 60 km, a 2–7 day wave manifests during the first 15 days of observation, and also a 3–4 day feature is present at the end of March and beginning of April. One should also note a 6.5–9.5 day wave periodicity over the 90–99 DY span. A 4 day component at 70 km appears in early March, and a 2–4 day component extends over mid March. Another wave of 4.5–7.5 day periodicity shows prevalence during the last half of March. During the 72–77 DY span, a 2–4 day wave component is evident at 80 km, as well as a 4–8 day wave that is prevalent around the ~81–93 DY interval. A wave of periodicity 4 days is also evident at the end of April. If we consider only the 3–4 day wave periodicity present during the initial 20 days of observations, then we can infer that the 3–4 day wave component over this site leads ahead of that of Gadanki (described previously) and also a third location in Africa (18° N, 30° E) (not shown here), which concludes that there is an eastward wave progression and supports the concept of UFK waves with a zonal wave number of 1.

To exclusively study the latitudinal extension of the observed 3–5 day component, the MLS temperature data at four altitudes over Gadanki and the observation site in North America are passed through a band-pass digital Bessel filter of cut offs at 3 and 5 days, centred around 4 days, after subtracting the means of the respective altitudes from each data point. The resulting filtered temperature deviation ($\Delta T$ in K) has been plotted in figure 4. The amplitude of oscillation increases with altitude, as indicated by the figure. From the plot, it is evident that $\Delta T$ over Gadanki is always much higher than that over North America for all the altitudes, which implies a lesser amplitude at higher latitude or latitudinal wave evanescence. This is another important property of the propagating UFK wave in the equatorial region. The readers should note another point that the behaviour of the UFK wave over Gadanki, as shown in the wavelet spectrums of figures 2 and 4 (red lines), exhibits some discrepancy or mismatch during

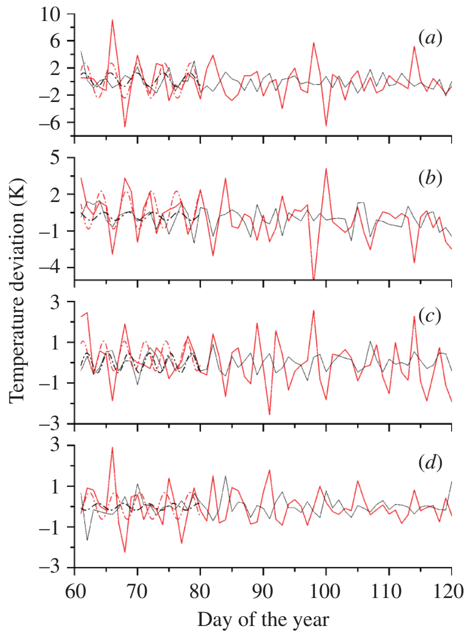


Figure 4. Filtered temperature deviation from mean ($\Delta T$ in K) of MLS after passing through a band-pass digital filter of bandwidth 3–5 days shown over Gadanki (red) and North America (black) at: (*a*) 80 km, (*b*) 70 km, (*c*) 60 km and (*d*) 50 km. The sinusoidal fit to the filtered data during 60–80 DY is also shown by dashed curves for Gadanki (red) and North America (black).

certain times of the observational span (although they match closely most of the time) because of different data platforms (ground based and satellite based).

## 4. Discussions

In our present work, we have shown the existence of 2–10 day periodicity Rossby planetary-scale waves. Our results of the observed parameters of the 3–5 day wave, i.e. period, vertical wavelength, eastward propagation and latitudinal evanescence, confirm the presence of the UFK wave in the mesosphere during the equinox time, which is generated in the troposphere and progresses upward. In addition, the eastward phase velocity is calculated from two observational sites (the phase difference is derived after fitting a least squares sinusoid to the filtered temperature in the range 60–80 DY for all four altitudes in figure 4 and taking the average of them) to be $\sim$140 m s$^{-1}$. The observed 5–7 day wave may be a 6.5 day wave as observed by Kovalam *et al.* (1999), Kishore *et al*. (2004) and Takahashi *et al*. (2006) and which we have not studied extensively enough to comment on. In addition to these, a quasi 2 day component is also observed in the spectra most of the time, which might be similar to the observations of Pancheva *et al.* (2004).

In this context, it is important to mention that the LiDAR has more uncertainty over the 80 km altitude due to a less backscattered signal that produces a lower signal to noise ratio at lower thermospheric regions. This discrepancy is evident in figure 1(*a*) through the large difference between the MLS and the LiDAR temperatures over several days in the present observations, and it has also been reported by previous investigators (Guharay *et al.* 2009, Mertens *et al.* 2009) using space-based Sounding of the Atmosphere using Broadband Emission Radiometry (SABER) and ground-based LiDAR data. Therefore, great care must be taken while performing quantitative analysis with the data within this region. It should be noted that in the present paper, we have only shown the presence of the probable UFK wave without performing any detailed characterization, e.g. for estimating the accurate amplitude of the UFK wave, and are inevitably required to separate out aliasing effects due to dominant atmospheric tidal components (diurnal, semidiurnal, etc.) from the actual wave component.

The KWs play an important role in driving westerly acceleration of QBOs by significant momentum deposition. It is confirmed from ground-based and the satellite-based observations that as the KW progresses from low to high latitude and altitude, the spectrum is broadened to some extent, giving rise to a shift in wave frequency and vertical wavelength to higher values (Wallace and Kousky 1968). In addition, this broadening causes filtering processes in the atmosphere by absorbing the low-frequency, slow components and allowing the high-frequency, fast waves to propagate upward up to the thermosphere (Garcia and Salby 1987). Recently, Salby *et al*. (2007) studied global-scale KW properties in the upper atmosphere with the help of a theoretical numerical model, and they concluded that the eastward propagating KW, starting from the troposphere, can reach up to the mesosphere and make significant alterations in the dynamics of that region. Our observed UFK wave is supposed to be a manifestation of the previously mentioned driving mechanisms.

Past investigations by Kovalam *et al*. (1999) have verified the longitudinal propagation characteristics of the UFK wave over Asia and the central Pacific region, and it was also inferred that the 6.5 day wave was actually a manifestation of an unstable mode of the planetary wave. It is interesting to mention that Yoshida *et al*. (1999) found intra-seasonal variation features in the observed UFK wave in the mesosphere–lower-thermosphere (MLT) region with long-term zonal wind data obtained from radiosonde and meteor radar. We cannot conclude such a pattern of variability of the UFK wave from our present investigations because of a limited dataset. Takahashi *et al*. (2002) observed 3.5 day periodicity KWs, along with a quasi 2 day Rossby gravity wave, in mesospheric airglow intensities from São João do Cariri, Brazil (7° S, 37° W) with a 1 year database, which matches nicely with our observations. In addition, Sridharan *et al*. (2002) obtained a 3.5 day wave with a zonal wave number of 1 in the equatorial mesopause region using MF radar wind data. Most recently, Takahashi *et al*. (2007) have shown signatures of the UFK wave with a vertical wavelength ~40 km in the equatorial ionosphere using ionospheric sounding of h'F, critical F2 region frequency variation, zonal winds of meteor radar and SABER temperature data, along with a 2 day wave in meridional wind. Finally, they concluded that the UFK component could remarkably alter the equatorial ionospheric evening uplift. The characteristics of our observed UFK wave show significant resemblance with the discussed studies of the previous investigators.

## 5. Conclusions

Our observations have detected an evident feature of the 3–5 day wave that is supposed to be a UFK wave. After its generation from the lower atmosphere, it progresses through the mesosphere. The present investigation is carried out by utilizing the ground-based LiDAR and the space-based MLS temperature data, with the help of wavelet and digital filter analysis, which have corroborated our contemplation of the UFK wave; nonetheless, little discrepancy is also observed in some of the cases. The concerned UFK wave shows a vertical wavelength ~40 km and a phase velocity ~140 m $s^{-1}$, with a zonal wave number of 1 and equatorial trapping. The obtained wave parameters confirm the existence of the equatorial UFK wave, and are in close agreement with that of available literature, as discussed in the previous section. In addition to this, a quasi 2 day component and a 5–7 day wave are revealed in our study, although they are not investigated further here. We suspect this 5–7 day wave to possibly be a propagating 6.5 day wave, which has been reported in the past by other observers.

**Acknowledgements**

The authors are grateful to the National Atmospheric Research Laboratory (NARL), Tirupati, India and the Microwave Limb Sounder (MLS) team for providing excellent quality data. The authors are grateful to anonymous reviewers for their constructive comments and suggestions.

## References

Abatzoglou, J.T. and Magnusdottir, G., 2006, Planetary wave breaking and nonlinear reflection: seasonal cycle and interannual variability. *Journal of Climate*, **19**, pp. 6139–6152.

Andrews, D.G., Holton, J.R. and Leovy, C.B., 1987, Middle atmosphere dynamics (New York, NY: Academic Press).

Cracknell, A.P. and Varotsos, C.A., 2007, The IPCC fourth assessment report and the fiftieth anniversary of Sputnik. *Environmental Science and Pollution Research*, **14**, pp. 384–387.

Fusco, A.C. and Salby, M.L., 1999, Interannual variations of total ozone and their relationship to variations of planetary wave activity. *Journal of Climate*, **12**, pp. 1619–1629.

Garcia, R. and Salby, M., 1987, Transient response to localized episodic heating in the tropics, part II: far-field behavior. *Journal of the Atmospheric Sciences*, **44**, pp. 499–530.

Guharay, A., Nath, D., Pant, P., Pande, B., Russell III, J.M. and Pandey, K., 2009, Middle atmospheric thermal structure obtained from Rayleigh LiDAR and TIMED/SABER observations: a comparative study. *Journal of Geophysical Research*, **114**, D18105, doi: 10.1029/2009JD011963.

Hauchecorne, A. and Chanin, M.-L., 1980, Density and temperature profiles obtained by LiDAR between 30 and 70 km. *Geophysical Research Letters*, **7**, pp. 565–568.

Hitchman, M.H. and Leovy, C.B., 1988, Estimation of Kelvin wave contribution to the semiannual oscillation. *Journal of Atmospheric Sciences*, **45**, pp. 1462–1475.

Holton, J.R., 1972, Waves in the equatorial stratosphere observed with Nimbus 5SCR. *Journal of Atmospheric Sciences*, **29**, pp. 368–375.

Holton, J., Alexander, M. and Boehm, M., 2001, Evidence for short vertical wavelength Kelvin waves in the Department of Energy–Atmospheric Radiation Measurement Nauru99 radiosonde data. *Journal of Geophysical Research*, **106**, pp. 20 125–20 129.

Kishore, P., Namboothiri, S.P., Igarashi, K., Gurubaran, S., Sridharan, S., Rajaram, R. and Ratnam, M.V., 2004, MF radar observations of 6.5-day wave in the equatorial mesosphere and lower thermosphere. *Journal of Atmospheric and Solar-Terrestrial Physics*, **66**, pp. 507–515.

Kovalam, S., Vincent, R.A., Reid, I.M., Tsuda, T., Nakamura, T., Ohnishi, K., Nuryanto, A. and Wiryosumarto, H., 1999, Longitudinal variations in planetary wave activity in the equatorial mesosphere. *Earth Planets and Space*, **51**, pp. 665–674.

Liu, H.-L., Roble, R.G., Taylor, M.J. and Pendleton, W.R., 2001, Mesospheric planetary waves at northern hemisphere fall equinox. *Geophysical Research Letters*, **28**, pp. 1903–1906.

Mertens, C.J., Russell III, J.M., Mlynczak, M.G., She, C.-Y., Schmidlin, F.J., Goldberg, R.A., Lopez-Puertas, M., Wintersteine, P.P., Picard, R.H., Winick, J.R. and Xu, X., 2009, Kinetic temperature and carbon dioxide from broadband infrared limb emission measurements taken from the TIMED/SABER instrument. *Advances in Space Research*, **43**, pp. 15–27, doi: 10.1016/j.asr.2008.04.017.

Pancheva, D., Mitchell, N.J. and Younger, P.T., 2004, Meteor radar observations of atmospheric waves in the equatorial mesosphere/lower thermosphere over Ascension Island. *Annales Geophysicae*, **22**, pp. 387– 404.

Salby, M.L., Matrosova, L. and Callaghan, P.F., 2007, Global Kelvin waves in the upper atmosphere excited by tropospheric forcing at midlatitudes. *Journal of Geophysical Research*, **112**, D06111, doi: 10.1029/2006JD007235.

Schwartz, M.J., Lambert, A., Manney, G.L., Read, W.G., Livesey, N.J., Froidevaux, L., Ao, C.O., Bernath, P.F., Boone, C.D., Cofield, R.E., Daffer, W.H., Drouin, B.J., Fetzer, E.J., Fuller, R.A., Jarnot, R.F., Jiang, J.H., Jiang, Y.B., Knosp, B.W., Kruger, K., Li, J.-L.F., Mlynczak, M.G., Pawson, S., Russell III, J.M., Santee, M.L., Snyder, W.V., Stek, P.C., Thurstans, R.P., Tompkins, A.M., Wagner, P.A., Walker, K.A., Waters, J.W. and Wu, D.L., 2008, Validation of the Aura Microwave Limb Sounder temperature and geopotential height measurements. *Journal of Geophysical Research*, **113**, D15S11, doi: 10.1029/2007JD008783.

Siva Kumar, V., Rao, P.B. and Krishnaiah, M., 2003, Lidar measurements of stratosphere-mesosphere thermal structure at a low latitude: comparison with satellite data and models. *Journal of Geophysical Research*, **108**, 4342, doi: 10.1029/2002JD003029.

Sridharan, S., Gurubaran, S. and Rajaram, R., 2002, Radar observations of the 3.5 day ultra-fast Kelvin wave in the low latitude mesopause region. *Journal of Atmospheric and Solar-Terrestrial Physics*, **64**, pp. 1241–1250.

Takahashi, H., Buriti, R.A., Gobbi, D. and Batista, P.P., 2002, Equatorial planetary wave signatures observed in mesospheric airglow emissions. *Journal of Atmospheric and Solar-Terrestrial Physics*, **64**, pp. 1263–1272.

Takahashi, H., Wrasse, C.M., Pancheva, D., Abdu, M.A., Batista, I.S., Lima, L.M., Batista, P.P., Clemesha, B.R. and Shiokawa, K., 2006, Signatures of 3–6 day planetary waves in the equatorial mesosphere and ionosphere. *Annales Geophysicae*, **24**, pp. 3343–3350.

Takahashi, H., Wrasse, C.M., Fechine, J., Pancheva, D., Abdu, M.A., Batista, I.S., Lima, L.M., Batista, P.P., Clemesha, B.R., Schuch, N.J., Shiokawa, K., Gobbi, D., Mlynczak, M.G. and Russell, J.M., 2007, Signatures of ultra fast Kelvin waves in the equatorial middle atmosphere and ionosphere. *Geophysical Research Letters*, **34**, L11108, doi: 10.1029/2007GL029612.

Torrence, C. and Compo, G., 1998, A practical guide to wavelet analysis. *Bulletin of American Meteorological Society*, **79**, pp. 61–78.

Varotsos, C., 1987, Quasi-stationary planetary waves and temperature reference atmosphere. *Meteorology and Atmospheric Physics*, **37**, pp. 297–299.

Varotsos, C., 2002, The southern hemisphere ozone hole split in 2002. *Environmental Science and Pollution Research*, **9**, pp. 375–376.

Varotsos, C., 2003, What is the lesson from the unprecedented event over Antarctica in 2002? *Environmental Science and Pollution Research*, **10**, pp. 80–81.

Varotsos, C., 2004a, Atmospheric pollution and remote sensing: implications for the southern hemisphere ozone hole split in 2002 and the northern mid-latitude ozone trend. In *Monitoring of Changes Related to Natural and Manmade Hazards using Space Technology, Advances in Space Research*, **33**, pp. 249–253.

Varotsos, C., 2004b, The extraordinary events of the major, sudden stratospheric warming, the diminutive Antarctic ozone hole and its split in 2002. *Environmental Science and Pollution Research*, **11**, pp. 405–411.

Vincent, R.A., 1993, Long-period motions in the equatorial mesosphere. *Journal of Atmospheric and Solar-Terrestrial Physics*, **55**, pp. 1067–1080.

Wallace, J.M. and Kousky, V.E., 1968, Observational evidence of Kelvin waves in the tropical stratosphere. *Journal of the Atmospheric Sciences*, **25**, pp. 900–907.

Wu, D.L., Hays, P.B. and Skinner, W.R., 1994, Observations of the 5-day wave in the mesosphere and lower thermosphere. *Geophysical Research Letters*, **21**, pp. 2733–2736.

Yoshida, S., Tsuda, T., Shimizu, A. and Nakamura, T., 1999, Seasonal variations of 3.0–3.8 day ultra-fast Kelvin waves observed with a meteor wind radar and radiosonde in Indonesia. *Earth Planets and Space*, **51**, pp. 675–684.